REGULAR ARTICLE

blood advances

A molecular circuit linking the BCR to the NAD biosynthetic enzyme NAMPT is an actionable target in Richter syndrome

Vincenzo G. Messana,[1,*] Amelia Fascì,[1,*] Nicoletta Vitale,[2] Matilde Micillo,[1] Matteo Rovere,[1] Noemi A. Pesce,[1] Claudio Martines,[3] Dimitar G. Efremov,[3] Tiziana Vaisitti,[1] and Silvia Deaglio[1]

[1]Laboratory of Functional Genomics, Department of Medical Sciences, and [2]Department of Molecular Biotechnologies and Health Science, University of Turin, Turin, Italy; and [3]Molecular Hematology Unit, International Centre for Genetic Engineering and Biotechnology, Trieste, Italy

Key Points

- BCR cross-linking activates a positive feedback loop including NAMPT and sirtuins and converging on AKT activation.
- PI3Kγ/δ and NAMPT inhibitors synergize in blocking AKT activation and induce apoptosis, with potent antitumor activity in RS-PDX models.

This works defines, to the best of our knowledge, for the first time a molecular circuit connecting nicotinamide mononucleoside phosphoribosyl transferase (NAMPT) activity to the B-cell receptor (BCR) pathway. Using 4 distinct xenograft models derived from patients with Richter syndrome (RS-PDX), we show that BCR cross-linking results in transcriptional activation of the nicotinamide adenine dinucleotide (NAD) biosynthetic enzyme NAMPT, with increased protein expression, in turn, positively affecting global cellular NAD levels and sirtuins activity. NAMPT blockade, by using the novel OT-82 inhibitor in combination with either BTK or PI3K inhibitors (BTKi or PI3Ki), induces rapid and potent apoptotic responses in all 4 models, independently of their mutational profile and the expression of the other NAD biosynthetic enzymes, including nicotinate phosphoribosyltransferase. The connecting link in the circuit is represented by AKT that is both tyrosine- and serine-phosphorylated by PI3K and deacetylated by sirtuin 1 and 2 to obtain full kinase activation. Acetylation (ie, inhibition) of AKT after OT-82 administration was shown by 2-dimensional gel electrophoresis and immunoprecipitation. Consistently, pharmacological inhibition or silencing of sirtuin 1 and 2 impairs AKT activation and induces apoptosis of RS cells in combination with PI3Ki or BTKi. Lastly, treatment of RS-PDX mice with the combination of PI3Ki and OT-82 results in significant inhibition of tumor growth, with evidence of in vivo activation of apoptosis. Collectively, these data highlight a novel application for NAMPT inhibitors in combination with BTKi or PI3Ki in aggressive lymphomas.

Introduction

Occurring in a minority of patients with chronic lymphocytic leukemia (CLL), Richter syndrome (RS) represents the transformation of the disease into an aggressive lymphoma.[1] In the great majority of cases, the histological presentation is that of a diffuse large B-cell lymphoma (DLBCL), even though cases with Hodgkin lymphoma histology have been described.[2] RS is, in most cases, clonally related to the preceding CLL phase, as inferred from genetic analysis of VDJ rearrangements.[3,4] Transformation of CLL into RS is correlated with the acquisition of novel genetic lesions, such as *TP53* or *CDKN2A* mutations, typically associated with transformation of hematological malignancies from indolent to aggressive.[3,5,6] The prognosis of patients with RS, particularly of those with a lymphoma clonally related

Submitted 14 September 2023; accepted 2 February 2024; prepublished online on *Blood Advances* First Edition 15 February 2024; final version published online 11 April 2024. https://doi.org/10.1182/bloodadvances.2023011690.

*V.G.M. and A.F. contributed equally to this study.

Data in this article can be accessed upon reasonable request to the corresponding author, Silvia Deaglio (silvia.deaglio@unito.it).

The full-text version of this article contains a data supplement.

to the preceding CLL, is dismal, with a median survival of just a few months.[7] Currently, there are no satisfactory therapeutic regimens for the treatment of these patients, even though several trials combining old and new drugs are ongoing. B-cell receptor (BCR) inhibitors, such as ibrutinib and acalabrutinib, have been initially used for patients with RS,[8,9] even though resistance rapidly develops. In addition, most patients with RS are likely to have been treated with BTK inhibitors during the CLL phase, limiting use of these drugs and raising the question of their role in the transformation and the development of resistance of RS cells.[10,11] BCL-2 inhibitor treatment has also been considered, usually in association with chemoimmunotherapy or with anti-CD20 antibodies.[12,13] A recent trial combining venetoclax with R-EPOCH achieved ~50% complete responses, and a study of venetoclax plus R-CHOP is ongoing.[14] In addition, it is important to explore new drugs or new combination strategies to achieve better and longer lasting responses.[15] Our laboratory has extensively worked on this topic, exploiting xenograft models derived from patients with RS (RS-PDX) that were established from 4 different patients with RS and that maintain a tight resemblance to the primary tumor.[16] We have analyzed the role of novel antibody drug conjugates targeting RS using tumor-specific antigens, such as ROR1,[17] or B-cell restricted targets, such as CD37.[18] We have also studied the effects of novel drug combinations, highlighting a synergy between the dual phosphoinositide 3-kinase γ/δ inhibitor duvelisib and BCL-2i.[19] Even though safety issues on the use of duvelisib have limited initial enthusiasm toward the drug, PI3Ki are being evaluated in different combinations in clinical trials for patients with RS (see clinical trials NCT03534323 and NCT03884998).

Nicotinamide mononucleoside phosphoribosyl transferase (NAMPT), the rate-limiting enzyme in the synthesis of nicotinamide adenine dinucleotide (NAD) from nicotinamide (NAM), is the NAD biosynthetic enzyme that most rapidly responds to heightened cellular metabolic needs.[20,21] NAMPT is overexpressed in several human cancers and is an attractive tumor target.[22] Even though inhibitors of NAMPT have been in clinical trials for many years now, they did not go beyond phase 2 due to significant toxicity and limited responses, attributed to compensatory NAD biosynthesis through alternative pathways.[23] Recently, OT-82, a small molecule with potent anticancer activity in hematological malignancies, was recognized as an effective NAMPT inhibitor, renewing interest in this target,[24-28] alone or in combination.[29,30]

This work originates from the observation that BCR cross-linking in CLL cells is followed by rapid NAMPT upregulation, suggesting that the 2 pathways are functionally linked.[31] Here, we demonstrate the existence of a positive feedback loop involving the BCR and NAMPT and converging on AKT. The translational implication, demonstrated using in vitro cultures and RS-PDX models, is that the simultaneous block of PI3K and NAMPT has synergic effects, widening the spectrum of possible combination therapies for patients with RS.

Methods

Reagents and antibodies

The full list of reagents and antibodies used is in supplemental Methods.

Treatment of RS cells

RS-PDX models were established and maintained as described.[16]

To activate BCR signaling, RS cells were treated with plate-bound immunoglobulin M (IgM; 10 μg/mL; Southern Biotech, Birmingham, AL). Duvelisib (Selleckchem, Aurogene, Rome, Italy) was used at 5 μM for the indicated time points, whereas OT-82 was used at 0.625, 1.25, and 2.5 nM, according to the model.

RNA extraction and quantitative reverse transcription polymerase chain reaction

Total RNA was extracted using the RNAse Plus Mini Kit (Qiagen, Hilden, Germany), retrotranscribed to complementary DNA using the High-Capacity cDNA Reverse Transcription Kit (ThermoFisher, Milan, Italy) and analyzed using the CFX384 Touch Real time detection system (Bio-Rad, Hercules, CA). All primers were from ThermoFisher. Gene expression levels were computed using the DDCT method.

Western blotting

Lysates were prepared as described[17]; proteins resolved by SDS-PAGE and transferred into a 0.2 μm nitrocellulose Trans-Blot Turbo Transfer membrane using the Trans-Blot Turbo Transfer System (all from Bio-Rad). The optical density of the bands was determined with the Image Lab 3.0 software (Bio-Rad).

Enzymatic assays

NAD and adenosine triphosphate (ATP) levels were measured using bioluminescent assay (NAD/NADH-Glo Assay and CellTiter-Glo Luminescent Cell Viability Assay, Promega, Milan, Italy). Both NAD and ATP levels were normalized over total protein levels (RLU × μL/μg). Sirtuin activity was evaluated using a fluorimetric assay (EPI018, Sigma-Aldrich, Milan, Italy) and normalized on protein levels (pmol/min per μg).

Apoptosis evaluation and combination index

Cell viability was determined by Annexin V-APC Apoptosis Kit (ThermoFisher). Samples were acquired by flow cytometry using FACSCelesta (BD Bioscience, Franklin Lakes, NJ) and analyzed with the FACSDiva (BD Bioscience) software.

Immunoprecipitation and 2D electrophoresis

Full details on immunoprecipitation and 2-dimensional (2D) gel electrophoresis are reported in supplemental Methods.

Gene silencing

For *SIRT1* and *SIRT2* silencing, freshly isolated RS cells (6×10^6) were transfected with validated siRNA for SIRT1 (sc-40986), SIRT2 (sc-40988), or scramble siRNA (sc-37007), from Santa Cruz Biotechnology (DBA Italia, Milan, Italy) using the NEPA21 Super Electroporator (Nepa Gene, Chiba, Japan). After transfection, RS cells were cultured in a complete medium and harvested at 24 hours for protein and RNA extraction or treated with duvelisib for 24 and 48 hours.

In vivo treatment

The Italian Ministry of Health approved all in vivo experiments (approval no. 571/2022-PR). RS cells (5×10^6) were resuspended

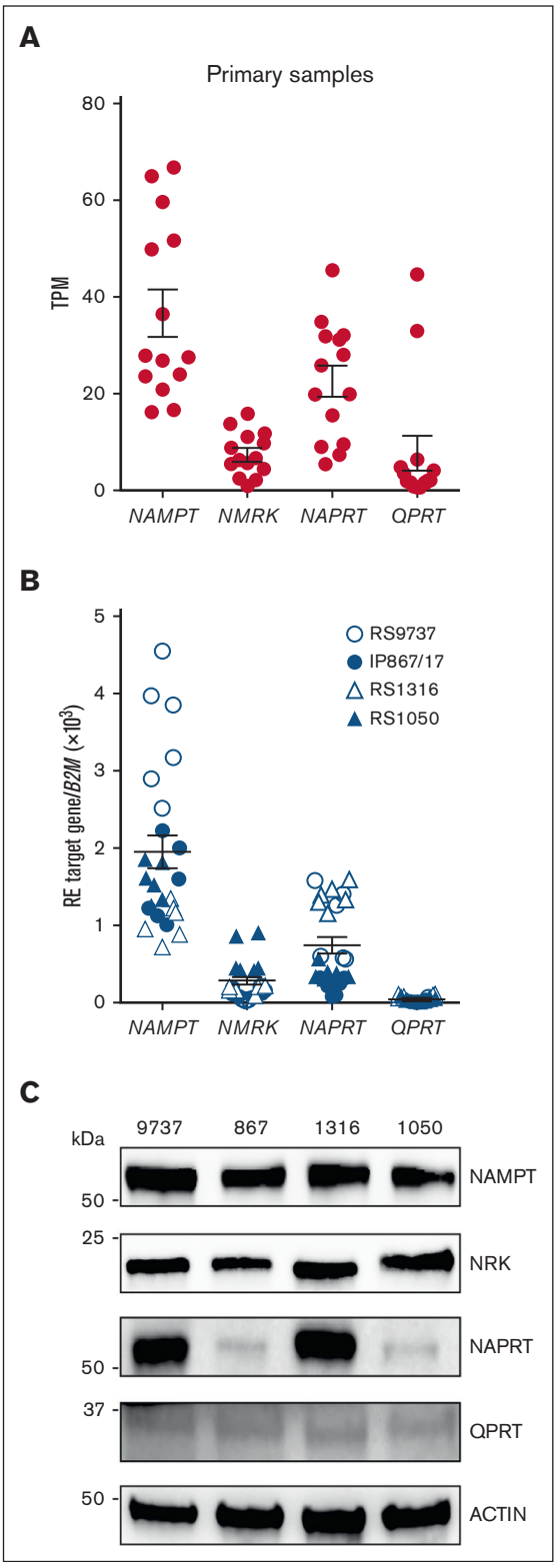

Figure 1. Expression of NBEs in RS primary samples and PDX models. (A) Expression of NBEs obtained from RNA-sequencing data in a cohort of 14 primary samples. Data report the expression as transcript per million reads (TPM) of *NAMPT*, *NMRK*, *NAPRT*, and *QPRT* as dot plots with mean ± standard error of the mean (SEM). (B-C) Quantitative reverse transcription polymerase chain reaction (qRT-PCR) analysis and western blot panels showing NBEs expression in 4 RS-PDX models (namely RS9737, IP867/17, RS1316, and RS1050) evaluated at different in vivo passages. mRNA expression was normalized over β-2-microglobulin (B2M). Actin was used as a loading control in western blot. NBE, NAD biosynthetic enzyme.

in RPMI-1640-Matrigel (1:1; Corning, Milan, Italy) and injected (double flank) into 8-week-old NOD/SCID/γ-chain$^{-/-}$ (NSG) mice and left to engraft. When a palpable mass was apparent, animals were randomly assigned to 4 different groups and treated with vehicle (5% dimethyl sulfoxide, 90% PEG300, and 5% Tween 80 or 30% hydroxypropyl-b-cyclodextrin; all from Sigma-Aldrich), duvelisib (100 mg/kg), OT-82 (40 mg/kg), or their combination. Treatment was administered by oral gavage for 3 consecutive days, followed by 4-day off, for a total of 3 cycles. Four days before treatment initiation, animals were put on a niacin-free rodent diet (Envigo, Bresso, Italy). During the whole experiment, mice were monitored and tumor masses were regularly measured twice a week by caliper. Mice were euthanized 2 days after the last treatment.

IHC

A portion of tumor masses was formalin-fixed and paraffin-embedded for immunohistochemistry (IHC). To evaluate apoptosis, an anticleaved Caspase-3 antibody was used, followed by an antimouse HRP-conjugated antibody and 3,3′-diaminobenzidine (EnVision System, Dako, Glostrup, Denmark). Slides were analyzed using an AXIO Lab.A1 microscope (Zeiss, Oberkochen, Germany), equipped with a Canon EOS600D reflex camera, and the images acquired using the ZoomBrowserEX software (Canon, Tokyo, Japan).

Statistical analyses

Statistical analyses were performed using GraphPad v 9.0 (GraphPad Software, La Jolla, CA). The statistical test used is indicated in all figure legends, along with the *P* values.

Results

Expression of NAD-synthesizing enzymes in primary RS cells and RS-PDX models

NAD is a vital molecule for regulating redox reactions, as well as the activity of intracellular and extracellular NAD-dependent enzymes. Its biosynthesis is controlled through the activity of 4 rate-limiting enzymes, namely (1) NAMPT, which controls the biosynthetic pathway from NAM; (2) nicotinamide riboside kinase (NRK), from nicotinamide riboside; (3) nicotinate phosphoribosyltransferase (NAPRT), from niacin; and (4) quinolinic acid phosphoribosyltransferase from tryptophan, considered the only de novo pathway. By using RNA-sequencing data from a cohort of 14 primary RS samples derived from patients with newly diagnosed disease (and referred to as primary RS samples) and 4 RS-PDX models (RS9737, IP867/17, RS1316, and RS1050), we showed that NAMPT is invariably expressed in all samples, whereas NRK and NAPRT display generally lower (NRK) and more variable (NAPRT) levels of expression (Figure 1A). Quinolinic acid phosphoribosyltransferase constitutive expression was low to undetectable, except for 2 primary samples, supporting the notion that de novo biosynthesis does not occur in lymphocytes.[32] RNA-sequencing

data were confirmed in RS-PDX samples both at transcript and protein levels (Figure 1B-C), highlighting high expression of NAMPT in all 4 models. Intriguingly, RS9737 and RS1316 cells also showed a high constitutive expression of NAPRT, an enzyme associated to intrinsic resistance to treatment with NAMPT inhibitors in different cancer models.[23]

NAMPT is dynamically modulated upon BCR signaling

We next investigated the effects of BCR activation on NAD biosynthetic enzyme expression in RS cells, using RS cells obtained from PDX mice and cultured for up to 4 days. Cross-linking of the BCR using plate-bound anti-IgM antibodies was followed by significant increase in NAMPT messenger RNA (mRNA) and protein levels after 24 hours of IgM stimulation (Figure 2A-B). Activation of the BCR pathway was confirmed by increased expression of both *CCL3* and *MYC*, known BCR targets (supplemental Figure 1A-B).[33] In these conditions no statistically significant change in *NMRK* and *NAPRT* expression levels could be observed, confirming that NAMPT is the enzyme that most responds to environmental needs (supplemental Figure 2).

NAMPT upregulation was completely inhibited by treating RS cells with the PI3Kγ/δ inhibitor duvelisib, used at the dose of 5 μM for 24 hours (Figure 2A-B), which effectively blocks BCR signaling, while failing to induce apoptosis (not shown).[19] As a further confirmation of the effects of BCR signaling inhibition on NAMPT mRNA and protein upregulation, we used the noncovalent and highly selective BTK inhibitor pirtobrutinib,[34] which inhibited BCR-driven NAMPT upregulation at the mRNA and protein levels (supplemental Figure 3A-B).

Consistent with NAMPT upregulation, cellular NAD levels were markedly increased 24 hours after BCR cross-linking compared with unstimulated cells in all 4 RS-PDX models (Figure 2C). Increased bioavailability of NAD levels fueled NAD-dependent sirtuins activity, as documented using a sirtuin activity assay (Figure 2D). Pretreatment of RS cells with duvelisib completely inhibited both NAD accumulation and sirtuin activity, demonstrating a specific linkage to BCR activation (Figure 2C-D). Inhibition of sirtuin activity was also documented after BCR blockade using pirtobrutinib (supplemental Figure 3C).

These findings highlight a molecular circuit connecting BCR activation to NAD biosynthesis through NAMPT upregulation, in turn, positively affecting the activity of NAD-dependent sirtuins.

Functional cooperation between NAMPT and PI3Kγ/δ inhibitors

We next evaluated the effects of NAMPT inhibitors in an ex vivo experimental setting. Briefly, RS cells, freshly purified from NSG animals, were plated in the presence of different doses of OT-82, with FK866 used as control. Drug escalation testing (from 0.625-10 nM) clearly showed a progressive decline in intracellular NAD levels, already highly significant at the lowest dose and at 24 hours (supplemental Figures 4A and 5A for OT-82 and FK866, respectively). Concomitantly, we observed a significant decrease in intracellular ATP levels. RS1050 and IP867/17 models showed a steeper decline in ATP and NAD levels than RS9737 and RS1316 (supplemental Figure 4B). These findings are indicative of the onset of apoptosis, which was already evident at 24 hours and reached maximal levels at 48 hours. With ~20% residual live cells after 72 hours, RS1050 and IP867/17 cells showed a more complete apoptotic response than RS9737 and RS1316, in which the percentage of live cells at the same time point was in the range of 55% and 75%, respectively (supplemental Figure 4C-D). This striking difference was recapitulated by FK866, which also induced marked apoptosis selectively in RS1050 and IP867/17, whereas RS1316 and RS9737 remained mostly vital (supplemental Figure 5C-D). A likely explanation for the different behavior lies in the expression of NAPRT, which can compensate for NAMPT block and is higher in RS1316 and RS9737, while almost absent in the other 2 models (Figure 1B-C).

We next asked whether blockade of the BCR signaling pathway could synergize with OT-82 in inducing apoptosis of RS-PDX cells. To this purpose, we combined the sublethal dose of 5 μM duvelisib with 0.625 nM for RS1050 and IP867/17 and 1.2 nM for RS9737 and RS1316 (Figure 3A). Exposure to the combination of PI3Ki and NAMPTi for 48 hours and 72 hours strongly reduced cell viability compared with either drug used alone (Figure 3A-B for 72 hours; supplemental Figure 6A for 48 hours). On average, viability in combined treatment samples dropped to 50% after 48 hours (supplemental Figure 6A) and to 20% after 72 hours (Figure 3A), without differences based on NAPRT expression. Accordingly, by calculating the combination index[35] of duvelisib and OT-82 cotreatment, we highlighted a strong synergic effect (combination index <1) in all RS-PDX models (Figure 3A). Analysis of the apoptotic machinery demonstrated higher levels of cleaved Caspase 3 and PARP in the combination treatment compared with single treatments (Figure 3B; supplemental Figure 6B). These results were confirmed by showing that FK866 was synergic with duvelisib in inducing apoptosis, as determined using the Bliss Independence model (supplemental Figure 7). These findings were reproduced by inducing BCR blockade using pirtobrutinib, which effectively synergized with OT-82 in the induction of apoptosis (supplemental Figure 8).

Taken together, these results highlight a synergy between agents that block BCR signaling and NAMPT inhibitors in RS cells in inducing apoptosis, independently of the underlying genetic lesions and of the expression of NAPRT.

PI3Ki and NAMPTi converge on AKT in fully blocking the BCR signaling

In examining potential convergence points to explain the synergy between PI3Ki and OT-82, we focused on AKT, a central effector in the BCR signaling pathway. To achieve full activation, AKT needs to be phosphorylated at serine 473 and threonine 398 residues, an event mediated by PI3K, and deacetylated at lysines 14 and 20 (K14/20), a second posttranslational modification regulated by sirtuins. AKT acetylation at these specific lysine residues suppresses its activity by preventing its PIP_3-mediated recruitment at the inner leaflet of the plasma membrane. SIRT-mediated deacetylation of K14/20 is therefore a necessary step for its activation.[36-38] Several studies have demonstrated how NAD depletion via NAMPT inhibition results in the decrease of PIP_3 binding and phosphorylated AKT levels.[37,39-42] For these reasons, we determined AKT activation levels after BCR cross-linking in the presence or absence of NAMPT and PI3K inhibitors.

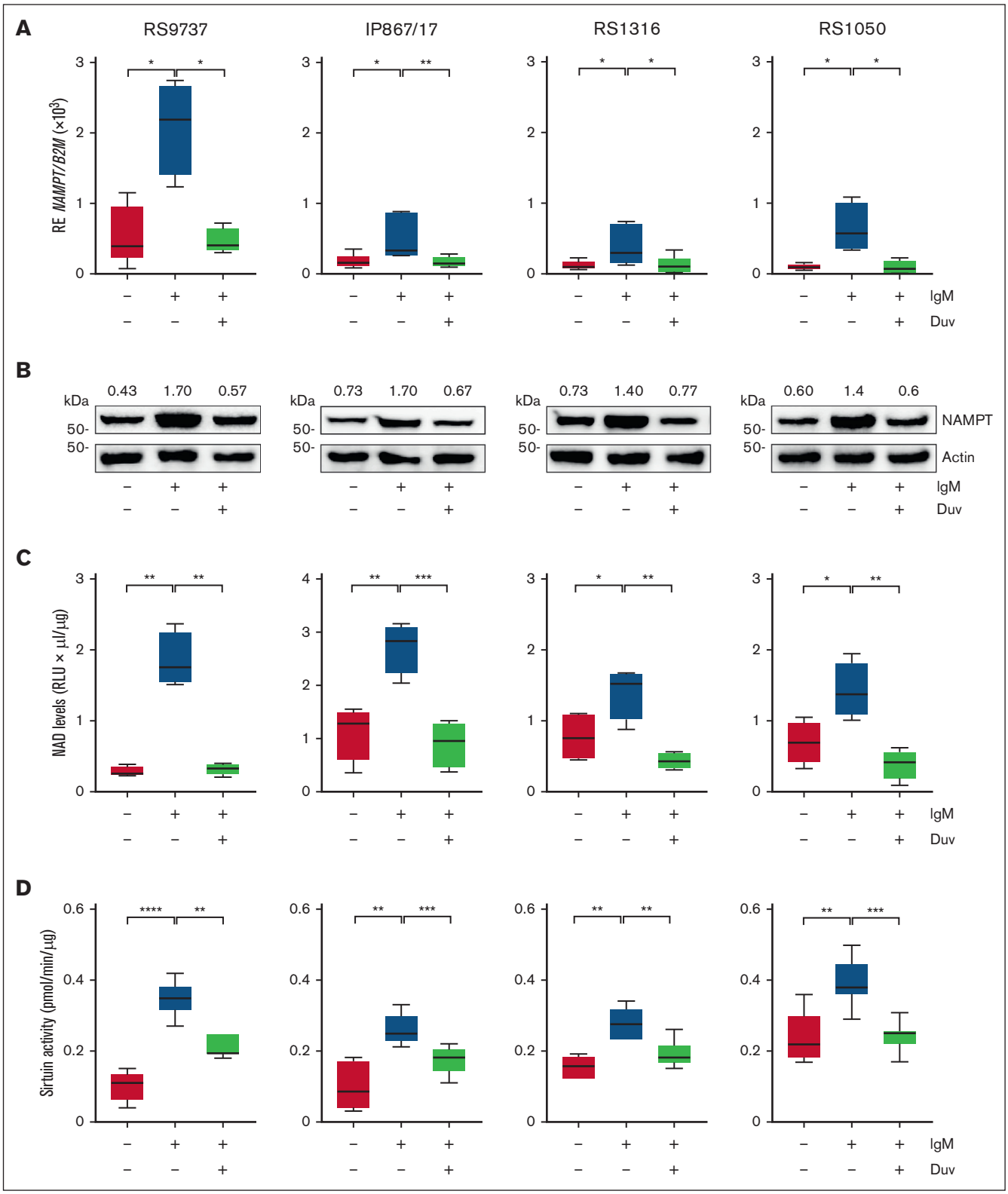

Figure 2. Signaling through the BCR increases expression and activity of NAMPT and sirtuins in RS cells. RS cells, freshly purified from tumor masses, were stimulated with a polyclonal anti-IgM for 24 hours to activate signaling. Duvelisib (5 microM) was added to block BCR activation, as indicated by the legend. (A) qRT-PCR analysis showing expression of *NAMPT* in RS cells. (B) Western blot data showing expression of NAMPT, in the conditions listed above. Band quantification values are indicated above them. (C) Box plots representing NAD levels measured through a luminescence assay, normalized on protein levels (RLU × µL/µg; ×10^4). (D) Sirtuin activity analysis in RS cells. The specific activity of sirtuins is represented as pmol/min per µg of proteins. All experiments were performed at least 5 times. Statistical analysis was performed using Student *t* test; *$P < .05$; **$P < .01$; ***$P < .001$; ****$P < .0001$.

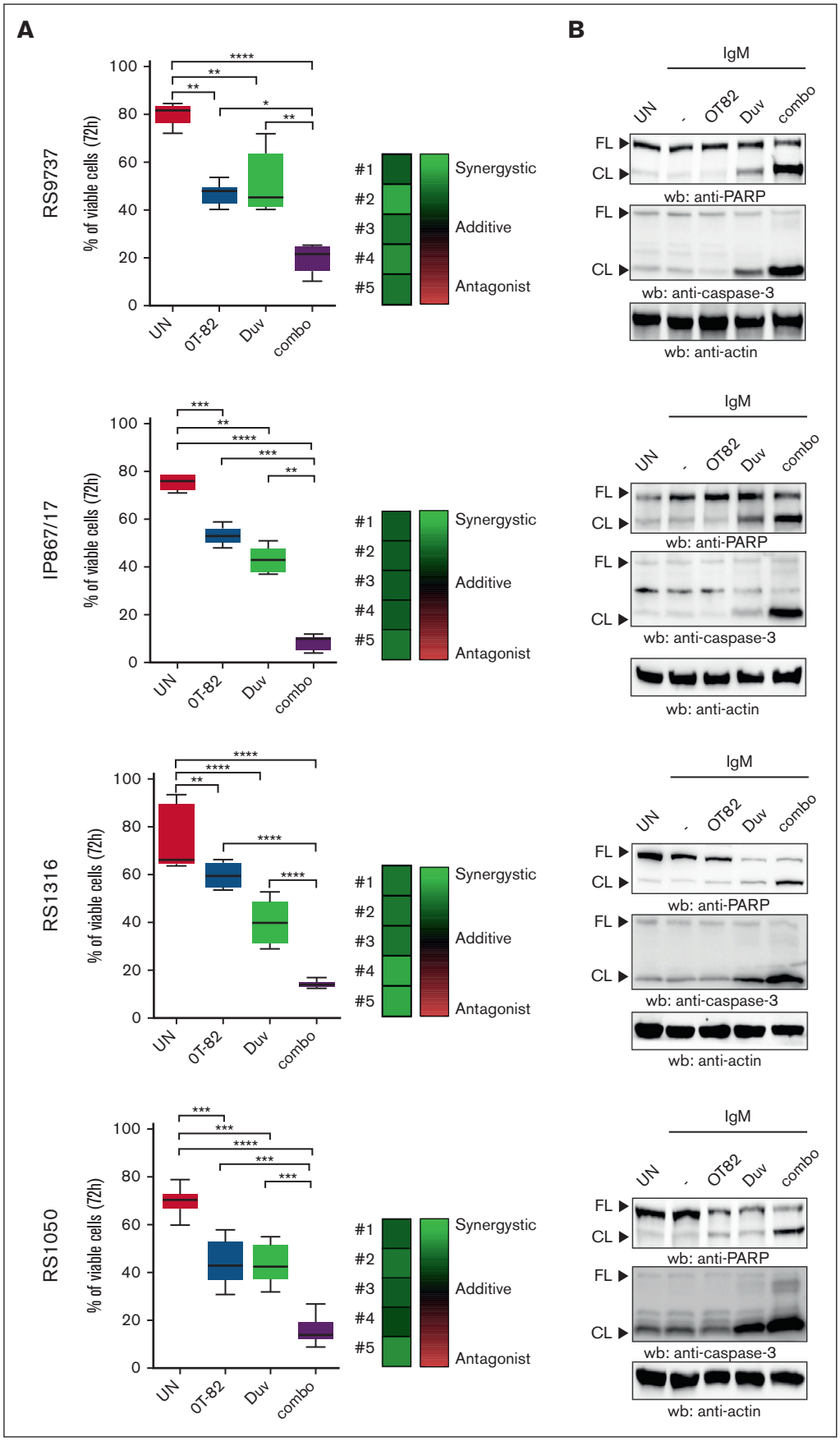

Figure 3.

As expected, upon BCR cross-linking, AKT was robustly phosphorylated both at Thr308 and Ser473 in all RS models, an event that was partially blocked by pretreatment with duvelisib and OT-82, whereas their combination achieved the highest effects (Figure 4A; supplemental Figure 9). Consistently, phosphorylation of GSK3b, which is directly downstream of AKT, was inhibited after combined treatment (Figure 4A; supplemental Figure 9).

To validate the hypothesis of a sirtuin-dependent activation of AKT, we performed immunoprecipitation experiments, followed by western blotting using an anti–acetyl-lysine antibody. At the baseline and upon IgM cross-linking, no AKT acetylation could be observed, whereas treatment with OT-82 was followed by accumulation of acetylated AKT, even more pronounced in the presence of trichostatin-A and NAM, used to completely block sirtuin activity (Figure 4B).[43] Therefore, fully activated AKT appears to be both deacetylated and phosphorylated. Evidence of multiple post-translational modifications was obtained using 2D IEF/SDS-PAGE electrophoresis and western blot for total AKT and demonstrating 4 AKT-immunoreactive spots: by using the acetyl-lysine blot signal, we identified the first one on the right as AKT without any post-translational modifications, the second one to singly modified AKT (either acetylated or phosphorylated), and the third and fourth as doubly- and triply-modified AKT molecules. As shown by the western blot in Figure 4C, the levels of p-AKT (both p-Thr308 and p-Ser473) decreased upon treatment and, at the same time, proteome-wide acetylation levels increased, shown by the increasing acetyl-α-tubulin signal. Correspondingly, in the 2D blot, we observed a shift in intensity upon treatment toward the spots on the left, which corresponds to AKT, either at a single or double lysine residue, corresponding to its inactive form. Trichostatin-A and NAM were again used as controls because they lead to complete inhibition of sirtuins activity and maximal acetylation, as confirmed by the intensity of the dot corresponding to acetylated alpha tubulin (Figure 4D).

SIRT1 or SIRT2 inhibition in combination with PI3Ki leads to increased apoptosis

AKT acetylation is regulated through the activity of SIRT1, which deacetylates AKT at K14/20, and SIRT2, which deacetylates AKT exclusively at K20.[36-38,44] Both these enzymes are expressed by primary RS cells and PDX models, as verified by RNA sequencing, quantitative reverse transcription polymerase chain reaction, and western blotting, with SIRT2 being the dominant enzyme, both in primary samples and in RS-PDX models (Figure 5A). Treatment of RS cells with either SIRT1-specific (Selisistat, EX-527) or SIRT2-specific (Thiomyristoyl) inhibitors triggered a potent apoptotic response after 48 hours (supplemental Figure 10A) and 72 hours of exposure, which was further increased by the addition of duvelisib (Figure 5B). In line with these findings, genetic knockdown of either SIRT1 or SIRT2, obtained using siRNAs, markedly reduced cell viability, particularly in the presence of duvelisib (Figure 5C; supplemental Figure 10B). In all instances, the combination of the 2 drugs was significantly more effective in inducing apoptosis than each drug used alone (Figure 5B). Consistently, exposure to the combination of a SIRT inhibitor and duvelisib completely blocked AKT activation, as documented by western blot (Figure 5D). Overlapping results were obtained after genetic silencing of both enzymes (Figure 5E; supplemental Figure 10B-D).

Combination of OT-82 and duvelisib shows antitumor properties in RS-PDX models

The efficacy of the PI3Ki/NAMPTi drug combination was then validated in vivo using RS-PDX models. RS cells were subcutaneously injected in 8-week-old NSG mice and left to engraft until tumor masses were at least 0.2 cm^3. Mice were then randomized in 4 groups and treated for 3 weeks with OT-82 (40 mg/kg), duvelisib (100 mg/kg), or their combination. A mixture of vehicles was used as the control. Treatments were administered for 3 consecutive days, leaving a 4-day washout period between cycles, as previously determined.[19,45] To increase the efficacy of OT-82 in vivo, 2 days before starting the treatment, regular mouse diet, supplemented with 115 mg/kg of niacin, was substituted with a custom diet containing 30 mg/kg of niacin, as previously described.[46] At the end of treatment, mice were euthanized and tumor masses recovered and measured. In line with in vitro results, it was clear that in all models, combination treatment was significantly more effective than individual treatments, as inferred by measuring volume and weight of the masses (Figure 6A for RS9737; supplemental Figures 11-13 for RS1316, RS1050 and IP867/17, respectively). We then performed flow cytometry–based apoptosis assays to show that the viability of RS-PDX cells was remarkably reduced in the masses treated with the drug combination (Figure 6B). NAD and ATP levels in the isolated RS-PDX cells showed drastic reduction after the combination of PI3Ki and NAMPTi, in line with the more robust apoptosis observed in these samples (Figure 6C). IHC assay for cleaved Caspase 3 on tumor masses confirmed a highly significant increase in staining of cleaved Caspase 3 in mice treated with the combination of the 2 drugs (Figure 6D). These in vivo results confirm how the combined use of these 2 drugs is much more effective than the individual treatments in reducing tumor progression.

Discussion

This work identifies, to the best of our knowledge, for the first time a possible therapeutic role for the NAMPT inhibitor OT-82 in PDX models of RS. NAMPT, the rate-limiting enzyme in the biosynthesis of NAD from NAM, has been an attractive tumor target for many years, considering its central role in supplying NAD upon increased metabolic needs of cells. However, the first inhibitor introduced in clinical trials, FK866, was unsuccessful because of both toxicity

Figure 3. The combination of duvelisib and OT-82 synergizes in inducing apoptosis in RS cells. (A) Graphs show percentage of viable cells, as determined by flow cytometry, after ex vivo incubation of RS cells for 72 hours with vehicle (UN), OT-82 (2.5 nM for RS9737 and RS136; 0.625 nM for RS1050 and IP867/17), duvelisib (Duv), or their combination (combo). The box plots show the median, interquartile range, and minimum and maximum values. Analysis of the combination index (CI) calculated using the Bliss Independence model to determine the effects of the OT-82 and Duv combination. Synergy is defined as CI <1 (green), whereas additive effect is CI ~1 (black), and antagonist effect is CI >1 (red). The individual squares refer to 5 independent experiments. (B) Expression levels of full length (FL) and cleaved (CL) Caspase 3 and PARP1 in RS cells after treatment with OT-82, Duv, or their combination (combo). Representative images from at least 3 independent experiments. Actin was used as loading control. Statistical analysis was performed using paired Student *t* test; **P* < .05; ***P* < .01; ****P* < .001; *****P* < .0001. UN, untreated.

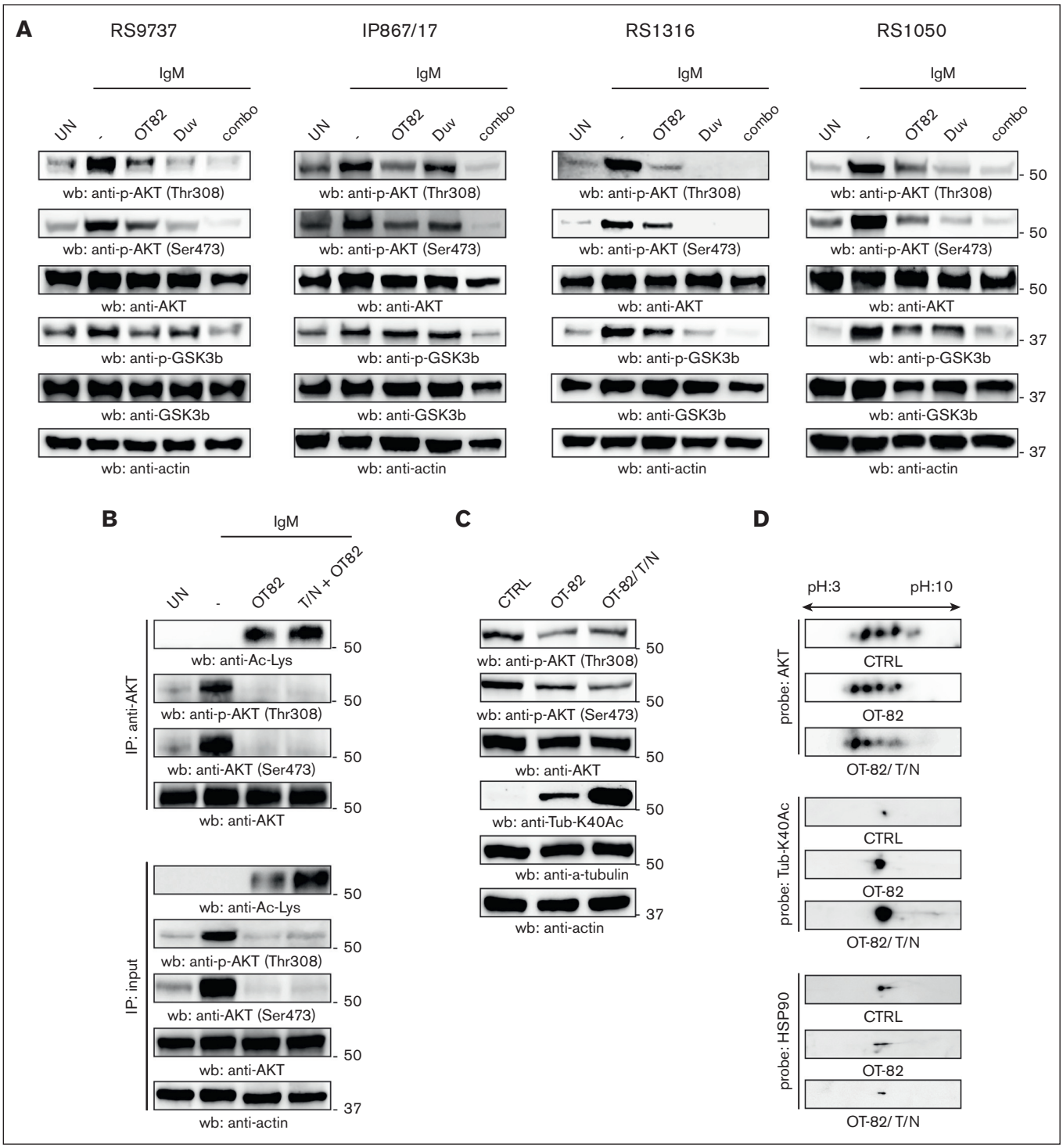

Figure 4. Synergy between PI3Ki and NAMPTi converges in downmodulating AKT signaling. (A) Activation status of AKT and GSK3β in RS cells after ex vivo stimulation of the BCR by cross-linking with a polyclonal anti-IgM antibody. When indicated, cells were pretreated for 24 hours with OT-82, Duv, their combo, or dimethyl sulfoxide (DMSO, shown in the figure as "-"). (B) Anti-AKT immunoprecipitation followed by immunoblotting with antiacetylated lysine, p-AKT(Thr308) or p-AKT (Ser473). An antitotal AKT antibody was used as control. Before lysis, RS cells were stimulated with polyclonal anti-IgM for 24 hours in the presence of a combination of OT-82 (0.625 or 2.5 nM), TSA (40 μM), and NAM (200 mM), or DMSO. Actin was used as a loading control in input samples. (C-D) IEF/SDS-PAGE 2D electrophoresis (D) followed by immunoblotting (C) with anti–p-AKT(Thr308), anti–p-AKT(Ser473), anti-AKT, and anti–acetyl-α-Tubulin. HSP90 and actin were used as loading controls in IEF/SDS-PAGE 2D and western blot, respectively. T/N, trichostatin A/nicotinamide (NAM); TSA, trichostatin A; UN, untreated.

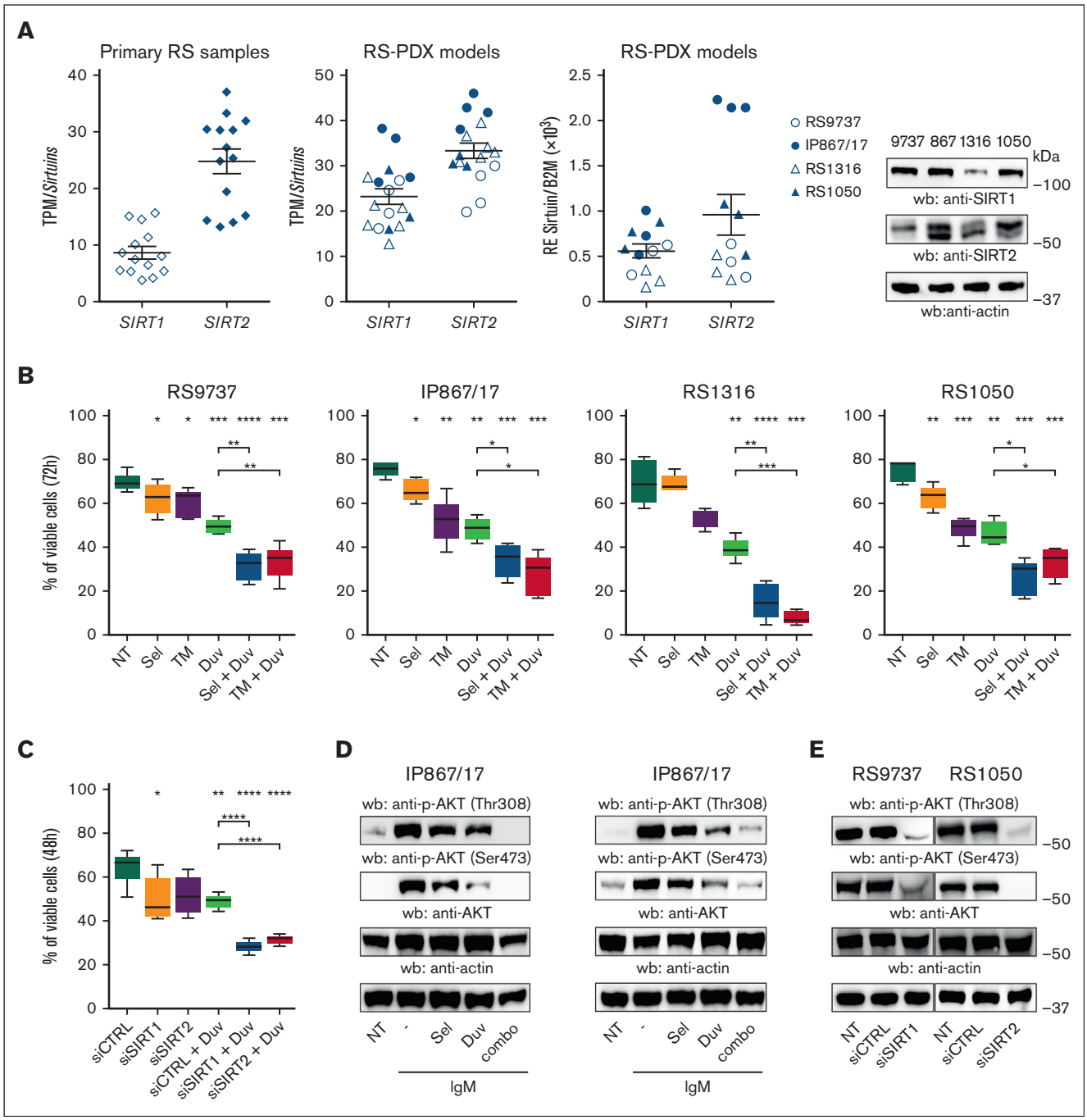

Figure 5. SIRT1/2 inhibition synergize with duvelisib in inducing apoptosis in RS-PDX cells. (A) Expression of *SIRT1* and *SIRT2* (depicted as TPM reads) obtained from RNA-seq data in a cohort of 14 primary patient samples and 4 RS-PDX models (RS9737, IP867/17, RS1316, and RS1050) taken at different passages. In qRT-PCR experiments shown in the third panel, mRNA was normalized over B2M. The fourth panel shows expression of SIRT1 and SIRT2 by western blot in RS-PDX models (RS9737, IP867/17, RS1316, and RS1050), with actin used as the loading control. (B) Percentage of viable RS cells after 72 hours treatment with vehicle (NT), selisistat (Sel), thiomyristoyl (TM), Duv, and their combination. Box plots of apoptotic data show the distribution of values: median, interquartile range, and minimum and maximum values. (C) Percentage of viable RS cells after nucleofection with short interfering RNA for SIRT1 (siSIRT1), SIRT2 (siSIRT2), or control (siCTRL) and then treated with Duv for 48 hours. Box plots of apoptotic data show the distribution of values: median, interquartile range, and minimum and maximum values. (D) Expression levels of p-AKT in RS cells stimulated for 24 hours with polyclonal anti-IgM and pretreated with Sel, TM, Duv, and their combination. Data were from at least 3 independent experiments. Actin was used as a loading control. (E) Expression levels of p-AKT after silencing of SIRT1 and SIRT2. Actin was used as a loading control. Statistical analysis was performed using paired Student *t* test; *$P < .05$; **$P < .01$; ***$P < .001$; ****$P < .0001$. NT, not treated.

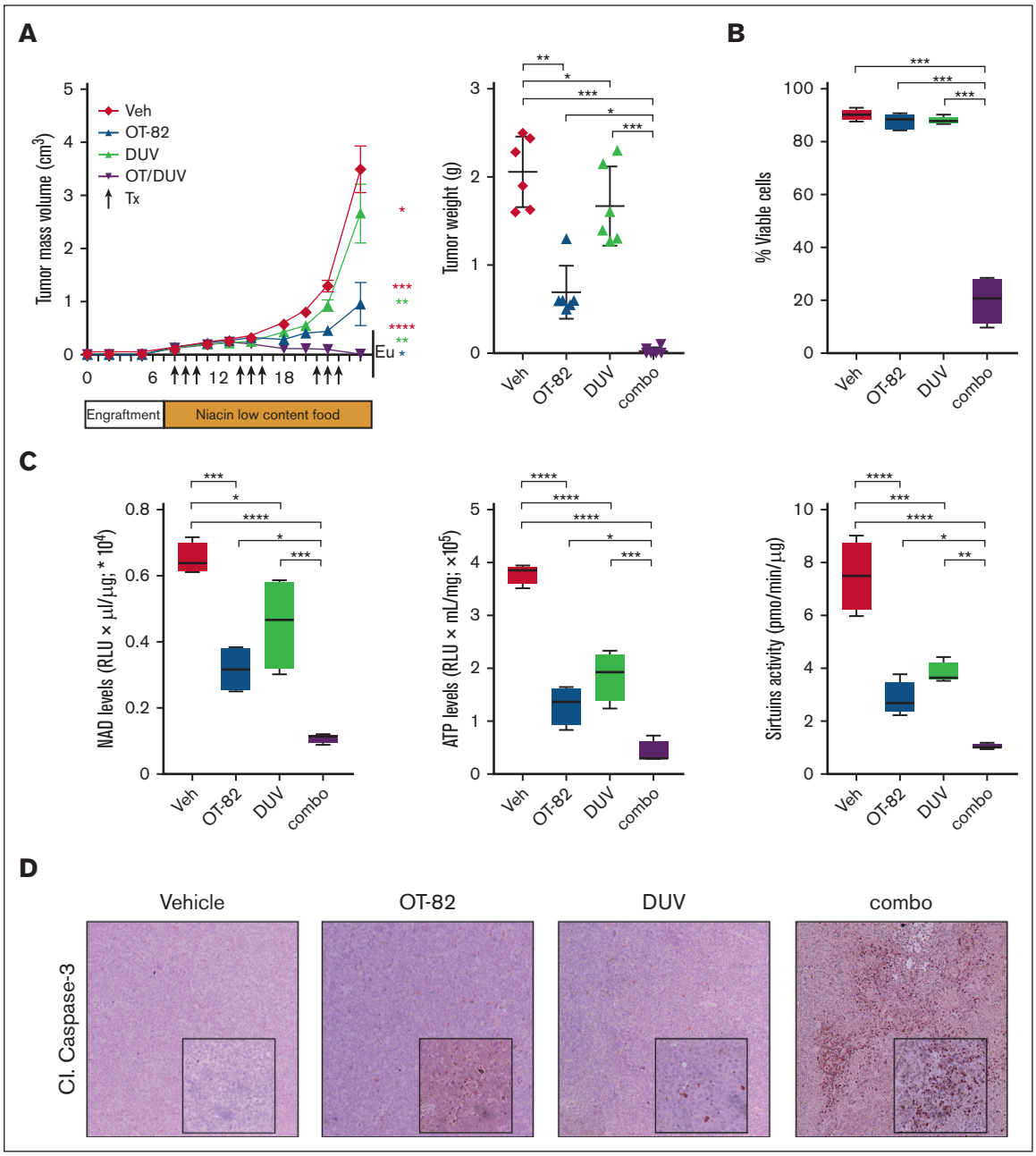

Figure 6. Tumor growth kinetics of RS9737 sc models treated with OT-82, duvelisib, and their combination. (A) RS cells were subcutaneously injected into both flanks of NSG mice. After palpable tumors were evident (tumor volume of 0.2 cm^3), animals were randomly assigned to vehicle, OT-82 40 mg/kg, duvelisib 100 mg/kg, or their combination. Two days before starting the treatment, regular mice diet was substituted with a low niacin diet. Drugs were administered by oral gavage for 3 consecutive days as indicated by arrows (Tx), leaving a 4-day washout period between treatment cycles. Tumor masses were measured using a digital caliper. Left panel displays mean and SEM values for tumor masses with data evaluated using the multiple sample paired *t* tests. Right panel displays individual mean and standard deviation values for tumor masses at the end of treatment on day 25. Data were evaluated using paired *t* tests. (B) Percentage of viable RS cells at the end of treatment with vehicle (Veh), OT-82, Duv, and their combo. Data are reported as mean ± SEM. (C) NAD levels, ATP levels, and sirtuin activity of RS cells at the end of treatment. NAD and ATP levels were normalized on protein content (RLU × µL/µg; ×10^4 and RLU × mL/mg; ×10^5, respectively). Sirtuin activity is represented as pmol/min per over µg of proteins. Statistical analysis was performed using a multiple Student *t* test; **P* < .05; ***P* < .01; ****P* < .001; *****P* < .0001. (D) Cleaved (Cl.) Caspase 3 as visualized by IHC performed on tumor masses (original magnification ×20 and ×40).

issues and lack of efficacy. Subsequent studies attributed lack of efficacy to expression of other NAD biosynthetic enzymes able to bypass NAMPT block and reconstitute NAD levels. Interest in NAMPT inhibitors, particularly for hematological cancers, was recently refueled by the introduction of the novel inhibitor OT-82, which has shown both tissue and cancer specificity in hematological tumors and no adverse effects in murine models of disease.[25,45]

In this work, we studied the effects of OT-82 in PDX models of RS,[16,17] which remains an orphan disease with no effective therapies. Analysis of the expression data, both in primary RS samples and RS-PDX models, of the 4 different NAD biosynthetic enzymes showed that NAMPT is significantly more expressed than the other enzymes, although its expression levels are heterogeneous. Importantly, upon BCR cross-linking, we observed a marked increase in NAMPT mRNA and protein levels in all RS-PDX models, confirming that this is the enzyme responsible for increased NAD production in the presence of anabolic signals. This behavior is unique to NAMPT because the expression of NAPRT and NMRK does not appear to be modulated by the activation or inhibition of BCR signaling in RS cells.[47,48] This finding highlights the existence of a connection between BCR signaling and transcriptional NAMPT upregulation, even though identification of the exact transcription factor involved is still lacking (Figure 7). Many of the effects stemming from NAMPT upregulation and the subsequent increase in NAD levels are mediated by the increase in the deacetylating activity of sirtuins on their protein targets.[48] From this perspective, NAMPT is considered the major regulator of sirtuin activity; not only does its activity generate NMN to start the recycling of NAM back to NAD, but it also acts as a scavenger of NAM itself, which acts as a sirtuin inhibitor. Sirtuins influence cellular responses to genomic instability by regulating cell cycle, DNA repair, cell survival, and apoptosis, thus having critical roles in cancer progression and metastasis.[49-53] Specifically, SIRT1 can induce chromatin silencing and regulates a wide variety of biological processes and cellular functions by deacetylating a large number of nonhistonic proteins, including AKT.[44] SIRT2 is also a key regulator of multiple physiological pathways. In the cytoplasm, in which it is predominantly localized, SIRT2 acts on a variety of substrates, including AKT.[38] Several different studies have highlighted the central role of SIRT1 and SIRT2 in hematological malignancies, and overexpression of SIRT1 and SIRT2 has also been reported in CLL and DLBCL, with elevated levels being associated with poor prognosis in CLL, AML, CML, and DLBCL.[54-58] Promising results have also been obtained from studies investigating the therapeutic potential of sirtuin inhibitors both in solid and hematological tumors. The SIRT1 inhibitor selisistat exhibited a strong antiproliferative effect in multiple leukemia cell lines,[59] whereas the antitumor activity of the SIRT1/2 inhibitor cambinol has been demonstrated on BCL6-expressing Burkitt lymphoma cells and xenografts.[60] Sirtinol treatment induced growth arrest and apoptosis in human breast cancer cells, lung cancer cells, and leukemic cells; and led to increased sensitivity to chemotherapy in prostate cancer cell lines.[41,61,62] Lastly, the SIRT2 inhibitor thiomyristoyl strongly reduced the viability of leukemic cell lines compared with nonhematopoietic cancer cell lines.[63] Together, these and other studies encourage the use of SIRT1 and SIRT2 inhibitors for solid and hematological cancers. However, the translation of in vitro and in vivo results into small molecule sirtuin inhibitors with the potential to be tested in clinical trials has been hampered by a variety of difficulties: the lack of isoform specificity, limited potency and bioavailability, and poor pharmacokinetics and pharmacodynamics of the candidates advanced to the trial stage.[64,65] In fact, no sirtuin inhibitor has been approved for the treatment of solid or hematological cancers. Some of the possible explanations are that sirtuins could be redundant in their actions, with significant overlaps in substrate specificity; or that, because some of their cellular roles are not

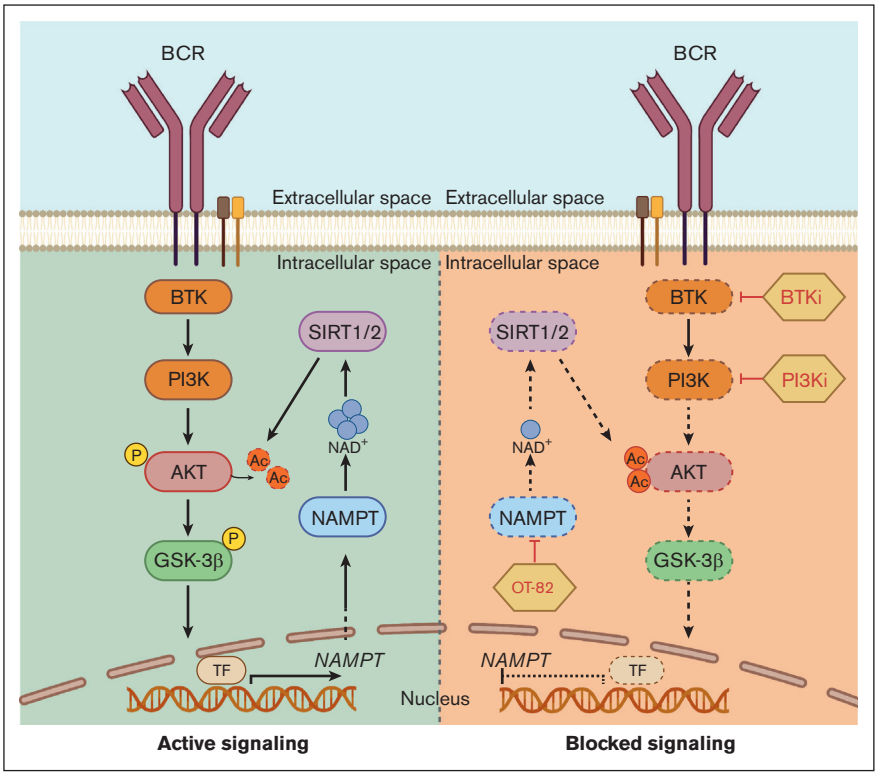

Figure 7. Representation of the molecular mechanism behind the synergy of action of BTKi or PI3K inhibitors and OT-82. Activation of the BCR receptor positively modulates the BTK-PI3K-AKT-NAMPT-SIRT1/SIRT2 axis. BTKi or PI3Ki treatment decreases AKT activation through inhibition of phosphorylation, whereas OT-82 inhibits its deacetylation through sirtuin blockade, interrupting a positive feedback loop.

dependent on enzymatic activity, enzymatic inhibition alone exhibits only moderate efficacy. It is reasonable to conceive that reducing NAD levels, by inhibiting NAMPT activity, could have a polypharmacological effect on the activity of the whole sirtuin family. In this study, we demonstrated the synergy arising from BCR signaling inhibitors, both at the BTK and PI3K level, combined with OT-82–mediated NAMPT inhibition (Figure 7). The dual treatment induces strong apoptosis in vitro in all the RS-PDX models tested. We also confirmed the same finding in vivo, observing a striking tumor regression in all RS-PDX models, independent of their genetic background. Importantly, we show that combined administration of duvelisib and OT-82 converges on AKT activation through the modulation of SIRT1/2 activity obtained by decreasing NAD levels. We also highlight the critical role that SIRT1 and SIRT2 play in RS cells, especially when they are targeted in combination with BCR signaling inhibition, either by pharmacological inhibition of their activities or by silencing their expression using siRNA. It must be noted that, although we corroborated the role of AKT in the synergy established between OT-82 and duvelisib, we cannot in principle exclude that the depletion of NAD through NAMPT inhibition could result in additional and yet to be defined effects. For example, SIRT1 and SIRT-2 has been reported to induce c-Myc overexpression, promoting tumor growth.[66-69]

In conclusion, our data emphasize the crucial nature of NAMPT as the main NAD biosynthetic enzyme and prove how NAD levels, especially in the context of BCR inhibition, are a potential metabolic Achilles heel of RS, which could be exploited therapeutically. NAMPT and BCR inhibitors cooperate in turning off central proneoplastic cellular pathways that promote RS proliferation and survival and their coadministration should be further investigated and potentially translated to clinical applications. Further studies are needed to determine whether these mechanistic observations may be clinically useful.

Acknowledgments

The authors thank Andrea Iannello and Elisabetta Bolli for technical help with the in vivo work. The authors also thank Oncotartis for providing OT-82 for part of the experiments.

This work was supported by the Associazione Italiana per la Ricerca sul Cancro (AIRC IG-23095 [S.D.] and MFAG 23107 [T.V.]) and by the Innovative Training Networks (ITN) INTEGRATA program (grant agreement 813284) (S.D.).

Authorship

Contribution: V.G.M. planned and performed experiments and contributed to manuscript writing; A.F. planned and performed experiments and together with S.D. organized text and figures; N.V., M.M., M.R., N.A.P., and C.M. performed experiments; D.G.E. and T.V. planned and critically reviewed experiments; and S.D. planned and interpreted experiments and wrote the manuscript.

Conflict-of-interest disclosure: The authors declare no competing financial interests.

ORCID profiles: M.R., 0000-0002-3260-4955; N.A.P., 0000-0002-5836-8575; C.M., 0000-0001-7136-7174; D.G.E., 0000-0001-9081-5462; S.D., 0000-0003-0632-5036.

Correspondence: Silvia Deaglio, Laboratory of Functional Genomics, Department of Medical Sciences, University of Turin, via Nizza 52, 10126 Turin, Italy; email: silvia.deaglio@unito.it.

References

1. Rossi D, Gaidano G. Richter syndrome: pathogenesis and management. *Semin Oncol*. 2016;43(2):311-319.
2. Rossi D, Spina V, Gaidano G. Biology and treatment of Richter syndrome. *Blood*. 2018;131(25):2761-2772.
3. Fabbri G, Khiabanian H, Holmes AB, et al. Genetic lesions associated with chronic lymphocytic leukemia transformation to Richter syndrome. *J Exp Med*. 2013;210(11):2273-2288.
4. Mao Z, Quintanilla-Martinez L, Raffeld M, et al. IgVH mutational status and clonality analysis of Richter's transformation: diffuse large B-cell lymphoma and Hodgkin lymphoma in association with B-cell chronic lymphocytic leukemia (B-CLL) represent 2 different pathways of disease evolution. *Am J Surg Pathol*. 2007;31(10):1605-1614.
5. Chigrinova E, Rinaldi A, Kwee I, et al. Two main genetic pathways lead to the transformation of chronic lymphocytic leukemia to Richter syndrome. *Blood*. 2013;122(15):2673-2682.
6. Klintman J, Appleby N, Stamatopoulos B, et al. Genomic and transcriptomic correlates of Richter transformation in chronic lymphocytic leukemia. *Blood*. 2021;137(20):2800-2816.
7. Condoluci A, Rossi D. Richter syndrome. *Curr Oncol Rep*. 2021;23(3):26.
8. Ten Hacken E, Gounari M, Ghia P, Burger JA. The importance of B cell receptor isotypes and stereotypes in chronic lymphocytic leukemia. *Leukemia*. 2019;33(2):287-298.
9. Gounari M, Ntoufa S, Apollonio B, et al. Excessive antigen reactivity may underlie the clinical aggressiveness of chronic lymphocytic leukemia stereotyped subset #8. *Blood*. 2015;125(23):3580-3587.
10. Ahn IE, Underbayev C, Albitar A, et al. Clonal evolution leading to ibrutinib resistance in chronic lymphocytic leukemia. *Blood*. 2017;129(11):1469-1479.
11. Kadri S, Lee J, Fitzpatrick C, et al. Clonal evolution underlying leukemia progression and Richter transformation in patients with ibrutinib-relapsed CLL. *Blood Adv*. 2017;1(12):715-727.
12. Bouclet F, Calleja A, Dilhuydy MS, et al. Real-world outcomes following venetoclax therapy in patients with chronic lymphocytic leukemia or Richter syndrome: a FILO study of the French compassionate use cohort. *Ann Hematol*. 2021;100(4):987-993.

13. Verdin E. NAD(+) in aging, metabolism, and neurodegeneration. *Science*. 2015;350(6265):1208-1213.
14. Davids MS, Rogers KA, Tyekucheva S, et al. Venetoclax plus dose-adjusted R-EPOCH for Richter syndrome. *Blood*. 2022;139(5):686-689.
15. Iannello A, Deaglio S, Vaisitti T. Novel approaches for the treatment of patients with Richter's syndrome. *Curr Treat Options Oncol*. 2022;23(4):526-542.
16. Vaisitti T, Braggio E, Allan JN, et al. Novel Richter syndrome xenograft models to study genetic architecture, biology, and therapy responses. *Cancer Res*. 2018;78(13):3413-3420.
17. Vaisitti T, Arruga F, Vitale N, et al. ROR1 targeting with the antibody-drug conjugate VLS-101 is effective in Richter syndrome patient-derived xenograft mouse models. *Blood*. 2021;137(24):3365-3377.
18. Vaisitti T, Vitale N, Micillo M, et al. Anti-CD37 alpha-amanitin conjugated antibodies as potential therapeutic weapons for Richter's syndrome. *Blood*. 2022;140(13):1565-1569.
19. Iannello A, Vitale N, Coma S, et al. Synergistic efficacy of the dual PI3K-delta/gamma inhibitor duvelisib with the Bcl-2 inhibitor venetoclax in Richter syndrome PDX models. *Blood*. 2021;137(24):3378-3389.
20. Rongvaux A, Shea RJ, Mulks MH, et al. Pre-B-cell colony-enhancing factor, whose expression is up-regulated in activated lymphocytes, is a nicotinamide phosphoribosyltransferase, a cytosolic enzyme involved in NAD biosynthesis. *Eur J Immunol*. 2002;32(11):3225-3234.
21. Houtkooper RH, Canto C, Wanders RJ, Auwerx J. The secret life of NAD+: an old metabolite controlling new metabolic signaling pathways. *Endocr Rev*. 2010;31(2):194-223.
22. Lin TC. Updated functional roles of NAMPT in carcinogenesis and therapeutic niches. *Cancers (Basel)*. 2022;14(9):2059.
23. Chowdhry S, Zanca C, Rajkumar U, et al. NAD metabolic dependency in cancer is shaped by gene amplification and enhancer remodelling. *Nature*. 2019;569(7757):570-575.
24. Kozako T, Aikawa A, Ohsugi T, et al. High expression of NAMPT in adult T-cell leukemia/lymphoma and anti-tumor activity of a NAMPT inhibitor. *Eur J Pharmacol*. 2019;865:172738.
25. Korotchkina L, Kazyulkin D, Komarov PG, et al. OT-82, a novel anticancer drug candidate that targets the strong dependence of hematological malignancies on NAD biosynthesis. *Leukemia*. 2020;34(7):1828-1839.
26. Mitchell SR, Larkin K, Grieselhuber NR, et al. Selective targeting of NAMPT by KPT-9274 in acute myeloid leukemia. *Blood Adv*. 2019;3(3):242-255.
27. Jones CL, Stevens BM, Pollyea DA, et al. Nicotinamide metabolism mediates resistance to venetoclax in relapsed acute myeloid leukemia stem cells. *Cell Stem Cell*. 2020;27(5):748-764.e4.
28. Gehrke I, Bouchard ED, Beiggi S, et al. On-target effect of FK866, a nicotinamide phosphoribosyl transferase inhibitor, by apoptosis-mediated death in chronic lymphocytic leukemia cells. *Clin Cancer Res*. 2014;20(18):4861-4872.
29. Khan HY, Uddin MH, Balasubramanian SK, et al. PAK4 and NAMPT as novel therapeutic targets in diffuse large B-cell lymphoma, follicular lymphoma, and mantle cell lymphoma. *Cancers (Basel)*. 2021;14(1):160.
30. Galli U, Colombo G, Travelli C, Tron GC, Genazzani AA, Grolla AA. Recent advances in NAMPT inhibitors: a novel immunotherapic strategy. *Front Pharmacol*. 2020;11:656.
31. Audrito V, Serra S, Brusa D, et al. Extracellular nicotinamide phosphoribosyltransferase (NAMPT) promotes M2 macrophage polarization in chronic lymphocytic leukemia. *Blood*. 2015;125(1):111-123.
32. Audrito V, Messana VG, Deaglio S. NAMPT and NAPRT: two metabolic enzymes with key roles in inflammation. *Front Oncol*. 2020;10:358.
33. Burger JA, Quiroga MP, Hartmann E, et al. High-level expression of the T-cell chemokines CCL3 and CCL4 by chronic lymphocytic leukemia B cells in nurselike cell cocultures and after BCR stimulation. *Blood*. 2009;113(13):3050-3058.
34. Aslan B, Kismali G, Iles LR, et al. Pirtobrutinib inhibits wild-type and mutant Bruton's tyrosine kinase-mediated signaling in chronic lymphocytic leukemia. *Blood Cancer J*. 2022;12(5):80.
35. Foucquier J, Guedj M. Analysis of drug combinations: current methodological landscape. *Pharmacol Res Perspect*. 2015;3(3):e00149.
36. Pillai VB, Sundaresan NR, Gupta MP. Regulation of Akt signaling by sirtuins: its implication in cardiac hypertrophy and aging. *Circ Res*. 2014;114(2):368-378.
37. Ramakrishnan G, Davaakhuu G, Kaplun L, et al. Sirt2 deacetylase is a novel AKT binding partner critical for AKT activation by insulin. *J Biol Chem*. 2014;289(9):6054-6066.
38. Cha Y, Kim T, Jeon J, et al. SIRT2 regulates mitochondrial dynamics and reprogramming via MEK1-ERK-DRP1 and AKT1-DRP1 axes. *Cell Rep*. 2021;37(13):110155.
39. Li Y, Ma X, Li J, et al. Corneal denervation causes epithelial apoptosis through inhibiting NAD+ biosynthesis. *Invest Ophthalmol Vis Sci*. 2019;60(10):3538-3546.
40. Oyarzun AP, Westermeier F, Pennanen C, et al. FK866 compromises mitochondrial metabolism and adaptive stress responses in cultured cardiomyocytes. *Biochem Pharmacol*. 2015;98(1):92-101.
41. Wang D, Hu Z, Hao J, et al. SIRT1 inhibits apoptosis of degenerative human disc nucleus pulposus cells through activation of Akt pathway. *Age (Dordr)*. 2013;35(5):1741-1753.
42. Qian B, Yang Y, Tang N, et al. M1 macrophage-derived exosomes impair beta cell insulin secretion via miR-212-5p by targeting SIRT2 and inhibiting Akt/GSK-3beta/beta-catenin pathway in mice. *Diabetologia*. 2021;64(9):2037-2051.

43. Audrito V, Vaisitti T, Rossi D, et al. Nicotinamide blocks proliferation and induces apoptosis of chronic lymphocytic leukemia cells through activation of the p53/miR-34a/SIRT1 tumor suppressor network. *Cancer Res*. 2011;71(13):4473-4483.
44. Sundaresan NR, Pillai VB, Wolfgeher D, et al. The deacetylase SIRT1 promotes membrane localization and activation of Akt and PDK1 during tumorigenesis and cardiac hypertrophy. *Sci Signal*. 2011;4(182):ra46.
45. Somers K, Evans K, Cheung L, et al. Effective targeting of NAMPT in patient-derived xenograft models of high-risk pediatric acute lymphoblastic leukemia. *Leukemia*. 2020;34(6):1524-1539.
46. Terakata M, Fukuwatari T, Kadota E, et al. The niacin required for optimum growth can be synthesized from L-tryptophan in growing mice lacking tryptophan-2,3-dioxygenase. *J Nutr*. 2013;143(7):1046-1051.
47. Tempel W, Rabeh WM, Bogan KL, et al. Nicotinamide riboside kinase structures reveal new pathways to NAD+. *PLoS Biol*. 2007;5(10):e263.
48. Ruggieri S, Orsomando G, Sorci L, Raffaelli N. Regulation of NAD biosynthetic enzymes modulates NAD-sensing processes to shape mammalian cell physiology under varying biological cues. *Biochim Biophys Acta*. 2015;1854(9):1138-1149.
49. Chen X, Sun K, Jiao S, et al. High levels of SIRT1 expression enhance tumorigenesis and associate with a poor prognosis of colorectal carcinoma patients. *Sci Rep*. 2014;4:7481.
50. Herranz D, Maraver A, Canamero M, et al. SIRT1 promotes thyroid carcinogenesis driven by PTEN deficiency. *Oncogene*. 2013;32(34):4052-4056.
51. Leko V, Park GJ, Lao U, Simon JA, Bedalov A. Enterocyte-specific inactivation of SIRT1 reduces tumor load in the APC(+/min) mouse model. *PLoS One*. 2013;8(6):e66283.
52. Yuan H, Wang Z, Li L, et al. Activation of stress response gene SIRT1 by BCR-ABL promotes leukemogenesis. *Blood*. 2012;119(8):1904-1914.
53. Alhazzazi TY, Kamarajan P, Joo N, et al. Sirtuin-3 (SIRT3), a novel potential therapeutic target for oral cancer. *Cancer*. 2011;117(8):1670-1678.
54. Li L, Osdal T, Ho Y, et al. SIRT1 activation by a c-MYC oncogenic network promotes the maintenance and drug resistance of human FLT3-ITD acute myeloid leukemia stem cells. *Cell Stem Cell*. 2014;15(4):431-446.
55. Sasca D, Hahnel PS, Szybinski J, et al. SIRT1 prevents genotoxic stress-induced p53 activation in acute myeloid leukemia. *Blood*. 2014;124(1):121-133.
56. Jang KY, Hwang SH, Kwon KS, et al. SIRT1 expression is associated with poor prognosis of diffuse large B-cell lymphoma. *Am J Surg Pathol*. 2008;32(10):1523-1531.
57. Kan Y, Ge P, Wang X, Xiao G, Zhao H. SIRT1 rs3758391 polymorphism and risk of diffuse large B cell lymphoma in a Chinese population. *Cancer Cell Int*. 2018;18:163.
58. Dal Bo M, D'Agaro T, Gobessi S, et al. The SIRT1/TP53 axis is activated upon B-cell receptor triggering via miR-132 up-regulation in chronic lymphocytic leukemia cells. *Oncotarget*. 2015;6(22):19102-19117.
59. Cea M, Soncini D, Fruscione F, et al. Synergistic interactions between HDAC and sirtuin inhibitors in human leukemia cells. *PLoS One*. 2011;6(7):e22739.
60. Heltweg B, Gatbonton T, Schuler AD, et al. Antitumor activity of a small-molecule inhibitor of human silent information regulator 2 enzymes. *Cancer Res*. 2006;66(8):4368-4377.
61. Ota H, Tokunaga E, Chang K, et al. Sirt1 inhibitor, Sirtinol, induces senescence-like growth arrest with attenuated Ras-MAPK signaling in human cancer cells. *Oncogene*. 2006;25(2):176-185.
62. Kojima K, Ohhashi R, Fujita Y, et al. A role for SIRT1 in cell growth and chemoresistance in prostate cancer PC3 and DU145 cells. *Biochem Biophys Res Commun*. 2008;373(3):423-428.
63. Jing H, Hu J, He B, et al. A SIRT2-selective inhibitor promotes c-Myc oncoprotein degradation and exhibits broad anticancer activity. *Cancer Cell*. 2016;29(5):767-768.
64. Curry AM, White DS, Donu D, Cen Y. Human sirtuin regulators: the "Success" stories. *Front Physiol*. 2021;12:752117.
65. Rajman L, Chwalek K, Sinclair DA. Therapeutic potential of NAD-boosting molecules: the in vivo evidence. *Cell Metab*. 2018;27(3):529-547.
66. Menssen A, Hydbring P, Kapelle K, et al. The c-MYC oncoprotein, the NAMPT enzyme, the SIRT1-inhibitor DBC1, and the SIRT1 deacetylase form a positive feedback loop. *Proc Natl Acad Sci U S A*. 2012;109(4):E187-196.
67. Mao B, Zhao G, Lv X, et al. Sirt1 deacetylates c-Myc and promotes c-Myc/Max association. *Int J Biochem Cell Biol*. 2011;43(11):1573-1581.
68. Marshall GM, Liu PY, Gherardi S, et al. SIRT1 promotes N-Myc oncogenesis through a positive feedback loop involving the effects of MKP3 and ERK on N-Myc protein stability. *PLoS Genet*. 2011;7(6):e1002135.
69. Liu PY, Xu N, Malyukova A, et al. The histone deacetylase SIRT2 stabilizes Myc oncoproteins. *Cell Death Differ*. 2013;20(3):503-514.